

## Supplementary Information

### **Straightforward background depletion enables transaminase solid-phase library screening**

*Matteo Planchestainer, Eimear Hegarty, Christian Heckman, Louise J. Gurlay and Francesca Paradisi\**

#### **Affiliations**

*University of Nottingham, School of Chemistry, University Park, Nottingham NG7 2RD, UK*

M. Planchestainer, E. Hegarty, C. Heckmann, F. Paradisi

*University of Bern, Department of Chemistry and Biochemistry, Freiestrasse 3, 3012 Bern, Switzerland*

F. Paradisi

*Structural Biology Unit, Dep. Biosciences, Università degli Studi di Milano, Via Celoria 26, 20133*

*Milano, Italy*

L. J. Gurlay

<b>Table of contents</b>	
<b>Supplementary Abbreviations</b>	3
<b>Supplementary methods</b>	
Materials	3
Library Generation	3
Solid phase screening	4
Expression and standard activity assay	4
Characterization of mutant variants with respect to wild-type HEWT	5
Biotransformations	5
Kinetic parameters	6
Enantiospecificity evaluation	6
Thermal stability	7
Crystallisation	7
Data Collection and Structure Determination	7
<b>Supplementary figures</b>	
Figure 1 "Optimised amino acceptor screening based on the ortho-xylylenediamine assay"	8
Figure 2 "Validation of the solid screening based on the ortho-xylylenediamine assay"	9
Figure 3 "Validation of the alternative reporter 4-nitrophenethylamine"	9
Figure 4 "The use of alternative amine donors during the depletion step"	10
Figure 5 "pH effect on enzyme activity"	10
Figure 6 "pH effect on enzyme stability"	11
Figure 7 "Temperature effect on enzyme activity"	12
Figure 8 "Temperature effect on enzyme stability"	13
Figure 9 "Determination of TOF"	14
Figure 10 "Determination of kinetic parameters"	14
Figure 11 "Location of the I176M and L306M mutations on the HEWT crystal structure"	15
Figure 12 "Thermal stability for HEWT WT, B2, C1"	16
Figure 13 "Domain composition of the HEWT crystal structure"	16
<b>Supplementary tables</b>	
Table 1 "Kinetic Parameters"	15
Table 2 "X-ray data collection, refinement and validation parameters"	17
<b>Supplementary notes</b>	17
<b>Supplementary references</b>	18
GC-FID Chromatograms	19

## Supplementary Abbreviations

HEWT	<i>Halomonas elongata</i> Aminotransferase
WT	Wild-Type
<i>E. coli</i>	<i>Escherichia coli</i>
LB	Lysogeny broth
o-Xyly	<i>ortho</i> -Xylylenediamine
IPTG	Isopropyl $\beta$ -D-1-thiogalactopyranoside
(S)-PEA	(S)-(-)-1-Phenylethylamine
HPLC	High Performance Liquid Chromatography
GC	Gas Chromatography
PCR	Polymerase Chain Reaction
IPA	Isopropylamine

## Supplementary methods

### Materials

The pHESPUC plasmid, harbouring the gene encoding WT HEWT was obtained as previously described.<sup>1</sup> Chemically competent *E. coli* cells (both XL10 gold and BL21(DE3) strains) were available in house. The random mutagenesis kit, GeneMorph II, was purchased from Agilent Technologies. Plasmid extraction and PCR purification kits were obtained from Thermo Fisher Scientific. Ketone substrates and amine reference standards were purchased from Fluorochem and Sigma-Aldrich. All other chemicals were obtained from Fisher-Scientific.

### Library generation

HEWT randomised libraries were created by amplification of the *spuC* gene, harboured inside the pHESPUC plasmid, using the GeneMorph II random mutagenesis kit (Agilent Technologies) and primers FWD-*spuC* (5'-AAAGGATCCGATGCAAACCAAGACTATCAGG-3') and REW-*spuC* (5'-AAAGAAATTCTCATGCGGTTGGCTCCTCTTGC-3'). Primers were designed to incorporate *Bam*HI and *Eco*RI restriction sites (underlined) at the 5' and 3' ends, respectively. Polymerase chain reaction was carried out according to the manufacturers protocol using the following PCR program: 2 min of initial denaturation at 95 °C and then 40 cycles of 30 s denaturation at 95 °C, 30 s annealing at 63 °C and 90 s elongation at 72 °C with a 10 min final extension time at 72 °C. After gel-purification, the PCR product was digested with *Bam*HI and *Eco*RI restriction enzymes, ligated with pRSETb (also digested with *Bam*HI and *Eco*RI) and used to transform *E. coli* XL10-Gold electrocompetent cells. The size of the libraries was estimated to be between 5000 and 6000 by plating sequential dilutions of transformed cells onto LB-agar plate (100  $\mu$ g/mL ampicillin), while the rest were grown overnight in 10 mL LB media supplemented with 100  $\mu$ M

ampicillin. The plasmid library was purified using the GeneJET Plasmid Mini-prep kit (Thermo Fischer Scientific) and stored at -20 °C. Sequencing of random clones confirmed the introduction a range of 5-16 base mutation per DNA sequence (including silent mutations) and 5-10 amino acid substitutions in the final protein sequence.

### **Solid phase screening**

80 µL of chemically competent *E. coli* BL21(DE3) cells were transformed with 500 ng of plasmid library. 200 µL of the transformed cells, diluted with LB media (1:10 dilution), were spread onto LB-plates (100 µg/mL ampicillin) with a nitrocellulose membrane (Protean BA85, GE Healthcare) on the surface and incubated overnight at 37 °C. Expression was induced by placing the membrane on a LB plate supplemented with 1 mM IPTG. The induction plate was then incubated for 8 hours at 37 °C. After expression the membrane was placed on a dialysis plate (10 mM Tris-HCl pH 8, 0.1 mM PLP, and 2% (w/v) agar) and incubated overnight at 4 °C. The background depletion step was performed by placing the membrane on filter paper soaked in phosphate buffer (50 mM, pH 8.0) containing 10 mM (S)-1-phenylethylamine and 1% (v/v) DMSO for 30 minutes at room temperature. Afterwards, the membrane was washed for 20 minutes at room temperature by transferring to filter paper soaked in 50 mM phosphate buffer, pH 8.0. The screening step was then conducted by placing the membrane on filter paper soaked in 50 mM phosphate buffer, pH 8.0 containing, 10% (v/v) DMSO, 10 mM *o*-xylylenediamine, and 10 mM of the target amino donor. From the first round of screening, positive colonies were isolated on the basis of an increased rate of darkening with respect to the WT colonies. Subsequently, the positive colonies were isolated and expressed in 10 mL of ZYP-5052 auto-induction medium.<sup>2</sup> The crude extract of each variant was tested for the conversion of *para*-nitroacetophenone using 50 eq. alanine and analysed by HPLC after 24 hours. The 24 hours conversion of each variant was compared with the WT and the best variants were individually expressed in 300 mL of ZYP-5052 auto-induction media, purified by IMAC, and tested for enhanced activity.

Alternatively, *para*-nitrophenethylamine was used instead of *o*-xylylenediamine; isopropylamine (50 mM) or cadaverine were used instead of (S)-PEA.

### **Expression and standard activity assay**

HEWT wild-type and mutant variants were expressed and purified by immobilised-metal affinity chromatography (IMAC) as reported previously.<sup>1</sup> Protein yields: WT 80 mg/L of media, A1 6 mg/L, B1 7 mg/L, B2 15 mg/L, B3 35 mg/L, C1 28 mg/L. The protein concentration was determined by absorbance at 280 nm using a calculated  $\epsilon$  of 62.8 mmol<sup>-1</sup> cm<sup>-1</sup> for a single subunit with mw 54.2 KDa (Xpasy Protparam).

Enzymatic activity was initially probed using a kinetic assay developed by Schätzle *et al.*<sup>3</sup> For X-ray

crystallography purposes, the wild-type and mutant variants were incubated overnight at 4 °C with 10% (w/w) TEV protease to cleave the His-tag. Gel-chromatography was carried out as a final purification step, exchanging the buffer to 20 mM Tris-HCl pH 8.

### **Characterization of mutant variants with respect to wild-type HEWT**

A full characterization of the B3 mutant was not undertaken as initial experiments concerning reaction velocities and molar conversions indicated high similarity to the B2 mutant.

### **pH effect on enzyme activity and stability**

Experiments to investigate the optimum pH for enzyme activity were performed using the spectrophotometric assay outlined above with some modifications.<sup>3</sup> In this case, a universal buffer (25 mM citric acid, 25 mM KH<sub>2</sub>PO<sub>4</sub>, 25 mM Tris, 12.5 mM Na<sub>2</sub>B<sub>4</sub>O<sub>7</sub>, and 25 mM KCl) was used instead of potassium phosphate buffer to cover a broad range of pH values (from pH 6 – 12). Similarly, pH stability experiments were performed in universal buffer. The purified enzyme was first diluted in universal buffer at the desired pH and stored at 4 °C for 60 minutes. After the incubation period, the residual enzyme activity was measured using the spectrophotometric assay described above.<sup>3</sup>

### **Temperature effect on enzyme activity and stability**

Experiments to investigate the optimum temperature for enzyme activity were performed using the spectrophotometric assay outlined above across a range of temperatures (from 25 °C to 60 °C).<sup>3</sup> For the stability experiment, the enzyme was stored in phosphate buffer 50 mM pH 8 in the presence of pyridoxal 5'-phosphate (PLP) 1 mM and incubated at the desired temperature for up to 24 hours. After the incubation period, the residual enzyme activity was measured using the spectrophotometric assay described above.<sup>3</sup>

### **Biotransformations**

For the substituted acetophenone substrates (**1a** to **2a**), batch reactions were performed in phosphate buffer (50 mM, pH 8.0, 10% (v/v) DMSO), containing 10 mM of the ketone substrate, 50 eq. of L-alanine, 0.1 mM PLP and 0.1 mg/mL (1.9 µM) of HEWT, in a total reaction volume of 200 µL. Similarly, for the small cyclic ketone substrates (**3a** to **6a**), batch reactions were performed in phosphate buffer (50 mM, pH 8.0, 10% (v/v) DMSO), containing 10 mM of the ketone substrate, 1 eq. of (S)-(-)-1-phenylethylamine, 0.1 mM PLP and 1 mg/mL (19 µM) of HEWT, in a total reaction volume of 1 mL. The reactions were incubated at 37 °C with gentle shaking for up to 24 hours. Samples (10 µL aliquots) were quenched with 0.2% HCL every 15 min for the first 60 min of reaction, followed by sampling after

2 h, 4 h, 6 h and 24 h, respectively. All samples were analysed using a HPLC equipped with a Waters X-Bridge column (C18, 3.5  $\mu$ m, 2.1 mm x 30.0 mm). The aromatic substrates and products were detected using a UV detector at 210 nm, 250 nm or 280 nm following a gradient run (A: 0.01 % Ammonia in water, B: Acetonitrile. Gradient: 0 min 5 % A 95 % B; 3.10 min 0 % A 100 % B; 3.50 min 0% A 100 % B; 3.51 min 95 % A 5% B; 4.50 min 95 % A 5% B) at 40 °C. The flow rate was maintained 0.8 mL/min. The retention times in minutes were confirmed by comparison with commercially available compounds: acetophenone (2.0 min), (S)-1-Phenylethylamine (1.9 min), *para*-NO<sub>2</sub>-acetophenone (2.1 min), (S)-*para*-NO<sub>2</sub>-phenylethylamine (1.9 min), *para*-CN-acetophenone (1.8 min), (S)-*para*-CN-phenylethylamine (1.6 min). The conversion was determined by exploiting a calibration curve, and TOFs determined by monitoring the initial reaction rates, considering only the linear part of the conversion curves (Supplementary Figure 9).

### Kinetic parameters

The kinetic parameters for the small cyclic ketones were obtained by measuring the initial velocities of the enzymatic reaction and curve fitting according to the Michaelis-Menten equation using GraphPad Prism 5 software (GraphPad Software, Inc) (Supplementary Figure 10). For ketones 3a to 6a, the activity assay was performed at pH 8.0, 30 °C, in the presence of 5 mM (S)-1-phenylethylamine, 0.1 mM PLP, various concentrations of the ketone (0.5 to 75 mM), 0.1 mM PLP, 0.5% (v/v) DMSO, and an appropriate amount of enzyme (0.1-0.5 mg/mL = 1.9-9.3  $\mu$ M). The activity was determined by measuring the production of acetophenone at 245 nm ( $\epsilon$  = 12.6 mM<sup>-1</sup> cm<sup>-1</sup>). All experiments were conducted in triplicate.

### Enantiospecificity evaluation

For the determination of enantioselectivity, batch reactions (1 mL total volume), were carried out as described in the biotransformation methods. After 24 hours, the reactions were basified with the addition of 5 M NaOH (100  $\mu$ L), followed by extraction with ethyl acetate (900  $\mu$ L). To facilitate enantiomeric separation and allow for GC analysis, the amine products were acetylated with the addition of triethylamine (5  $\mu$ L) and acetic anhydride (5  $\mu$ L). For analysis of the small cyclic amines, the reaction mixtures were saturated with NaCl prior to basification and extracted with a 3:1 mixture of isopropanol and chloroform (2  $\times$  500  $\mu$ L). The amine products were then acetylated as described above. The samples were analysed by GC-FID using a Thermo Scientific™ Trace™ 1310 GC equipped with an Agilent CHIRASIL-DEX CB (25 m x 0.25 mm x 0.25 mm) column. The following method was used: injector temperature 230 °C, split ratio 1:10, continuous flow 1.7 mL/min: 40 °C for 2 min, 20 °C/min to 150 °C, hold for 5 min, then 30 °C/min to 225 °C, then hold for 8 min, FID temperature 250 °C. Helium was used as carrier gas. The retention times in minutes were: (S)-*para*-NO<sub>2</sub>-phenylethylamine (20.893

min), (*R*)- *para*-NO<sub>2</sub>-phenylethanamine (21.098 min), (*S*)-*para*-CN-phenylethanamine (18.150 min), (*R*)-*para*-CN-phenylethanamine (18.277 min), (*S*)-tetrahydrothiophen-3-amine (13.473 min), (*R*)-tetrahydrothiophen-3-amine (13.532 min), (*R*)-tetrahydrofuran-3-amine (10.135 min), (*S*)-tetrahydrofuran-3-amine (10.215 min), (*S*)-1-methylpyrrolidin-3-ylamine (10.032 min), (*R*)-1-methylpyrrolidin-3-ylamine (10.240 min), (*S*)-1-methyl-piperidin-3-ylamine (10.840 min), (*R*)-1-methyl-piperidin-3-ylamine (11.150 min). The enantiomeric purity was determined by comparison with commercially available compounds.

### Thermal stability

10 µL of each enzyme variant (6.5 mg/ml) were mixed with 10 µL SyproOrange solution (diluted 1:500 from the Sigma-Aldrich stock solution) and 6 µL 1M Tris-HCl pH 7.0 or 8.0, and the volume adjusted to 50 µL with deionised water. Three aliquots of 15 µL from each enzyme variant (for triplicate measurements) were transferred to 250 µl thin-walled white polypropylene PCR tubes (BioRad). The tubes were closed with clear caps and placed in MiniOpticon Real-time thermocycler (BioRad). Unfolding was measured by a corresponding increase in fluorescence intensity (excitation wavelength = 470-505 nm; emission = 540 nm-700 nm) that arises in response to the binding of SyproOrange to internally-located hydrophobic residues of the protein that become exposed during denaturation. A heat gradient of 20-99°C, increasing at a rate of 2°C/min was applied, and triplicate measurements were recorded for each sample. The final melting temperature ( $T_m$ ) was calculated from the negative derivative of the melting curves and as an average of triplicate values.

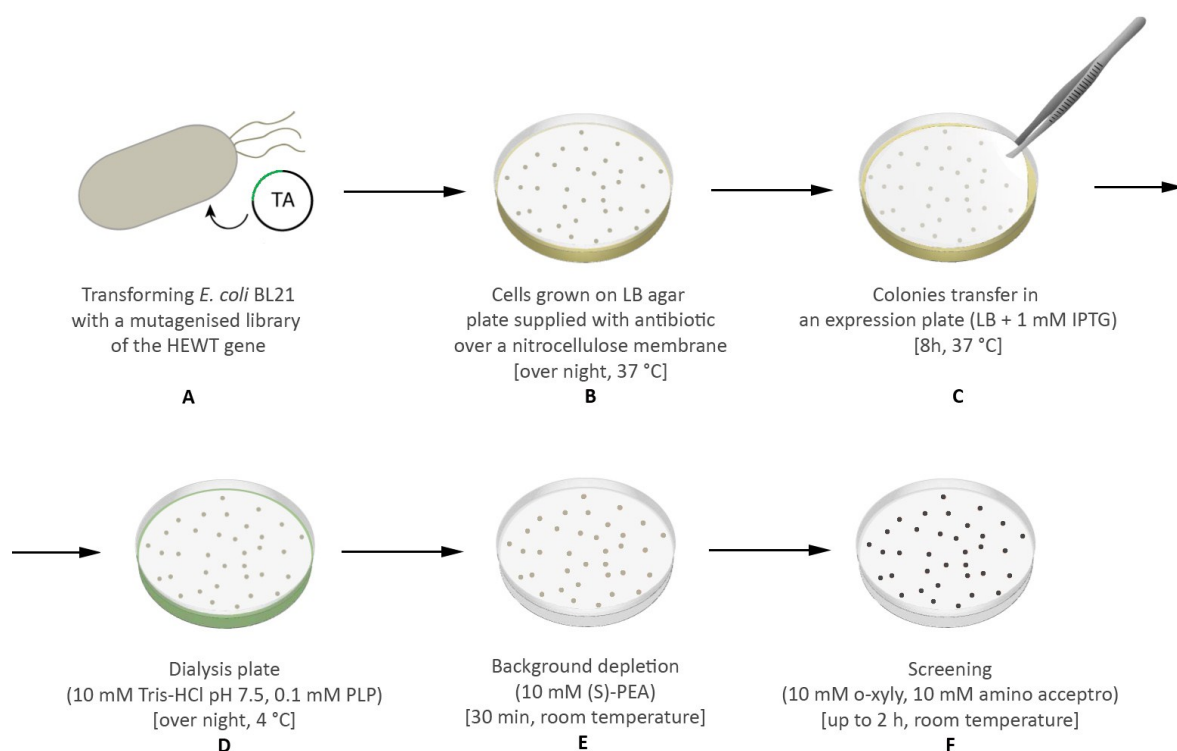
### Crystallisation

400 nL crystallisation drops of HEWT protein solution (6.5 mg/mL in 20 mM Tris-HCl, pH 8.0, containing 2 mM dithiothreitol (DTT) and 50 µM PLP) were set-up in 96-well round-bottomed sitting drop plates (Greiner), containing 100 µL of 96 different PEG/Ion screen conditions (Hampton Research). Three different protein concentrations were assessed, varying the amount of protein (30, 50 and 70 %) in the drop. A single crystal grew in a drop comprising 30% HEWT and PEG/Ion condition 25 (20% (*w/v*) PEG 3350, 0.2 M magnesium acetate, pH 7.9). The HEWT crystal was cryoprotected in a solution containing increased precipitant (25% PEG 3350), 0.1 M Tris-HCl pH 7.9 and 30 % (*v/v*) ethylene glycol, prior to cryocooling in liquid nitrogen.

### Data Collection and Structure Determination

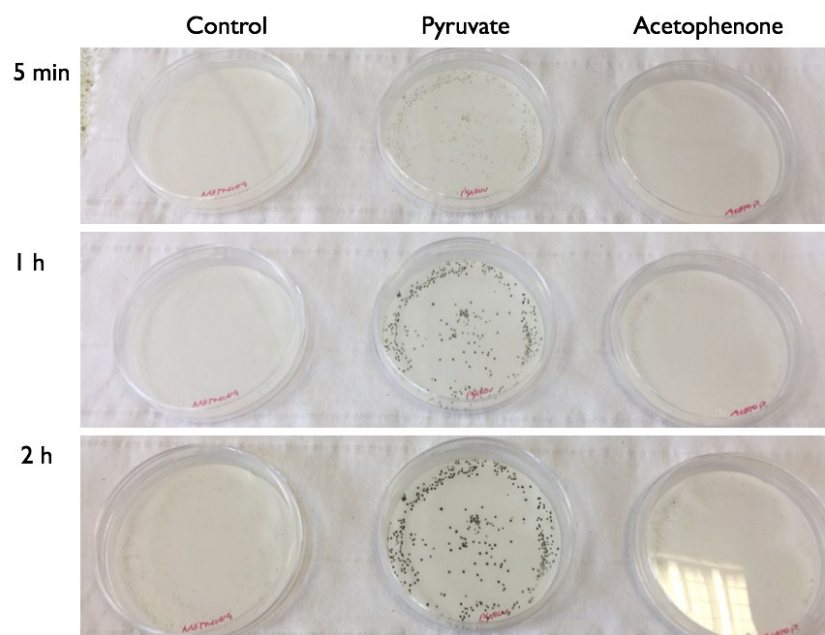
X-ray diffraction data were collected at 2.0 Å resolution on a single HEWT crystal at the automated MASSIF-1 beamline at the European Synchrotron Radiation Facility (ESRF, Grenoble, France).<sup>4,5</sup> Data

were processed using XDS<sup>6</sup> and assigned to a triclinic (P1) space group using POINTLESS and scaled using SCALA; both implemented in the CCP4i suite.<sup>7,8</sup> The 3D structure of HEWT was solved using Molrep and the structure of an aspartate aminotransferase from *Pseudomonas aeruginosa* (PDB entry 5TI8; 43% sequence identity over 433 aligned residues) as a search model.<sup>9</sup> The structure was manually built using COOT and refined using phenix.refine until satisfactory refinement parameters were achieved ( $R_{\text{work}} = 16\%$ ;  $R_{\text{free}} = 21.0\%$ ).<sup>10,11</sup> All residues are located in allowed regions of the Ramachandran except for Ala283 in both chains and Lys284 (chain A); the catalytic lysine is often found as an outlier in many PLP-dependent enzymes due to its covalent interaction with PMP. Data collection parameters and refinement statistics are shown in Supplementary Table 3.

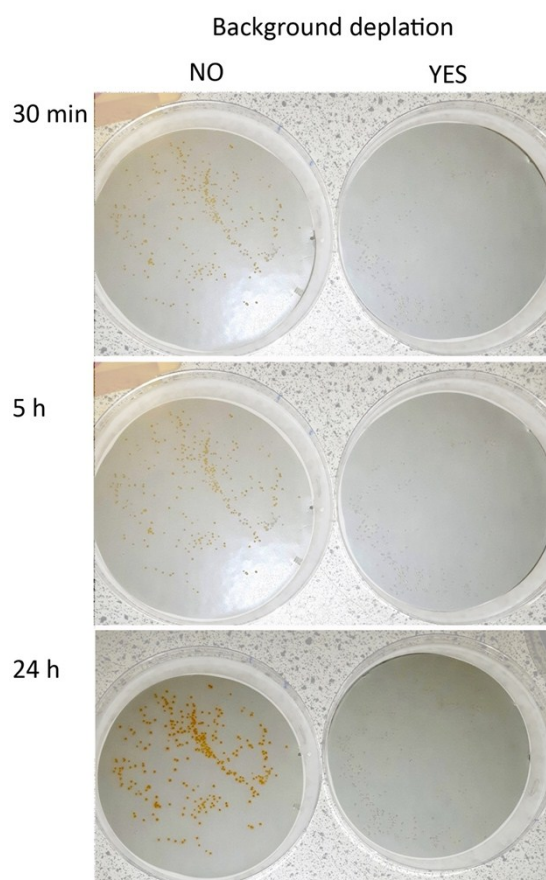


**Supplementary Figure 1 | Optimised amino acceptor screening based on the *ortho*-xylylenediamine assay.** *E. coli* BL21(DE3) cells are transformed with the HEWT library of interest (**A**) and colonies are grown overnight on a nitrocellulose membrane placed on LB agar plates supplemented with 100  $\mu\text{g}/\text{mL}$  of ampicillin (**B**). Membranes are transferred to LB agar plates supplemented with 100  $\mu\text{g}/\text{mL}$  of ampicillin and 1 mM IPTG for protein expression for 8 hours (**C**). To minimised false positive background colour formation and to stop the cell metabolism, colonies are dialyzed overnight by transferring the membrane to a dialysis plate containing 2% agar, 10 mM Tris-HCl pH 8, and 0.1 mM PLP (**D**). Afterwards, the background is depleted by placing the membrane on filter paper soaked in 10 mM (S)-1-phenethylamine in phosphate buffer pH 8, 1% (v/v) DMSO for 30 minutes (**E**). Finally, screening is conducted by incubation of the membranes on assay plates containing 10 mM *ortho*-xylylenediamine and 10 mM amino acceptor of interest in phosphate buffer pH 8, 10% (v/v) DMSO (**F**). Scheme elaborated from Weis *et al.*<sup>12</sup>

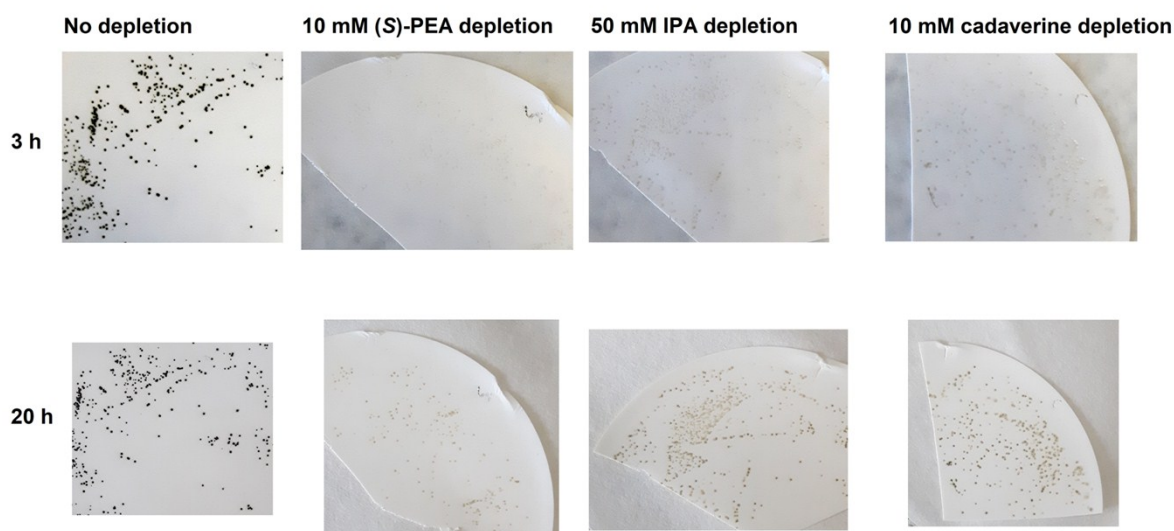




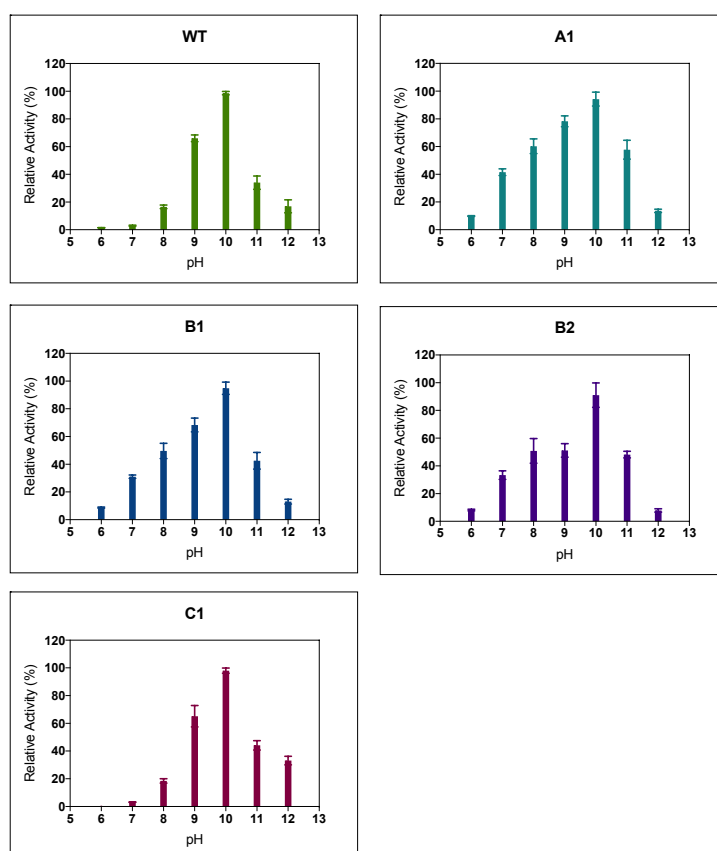
**Supplementary Figure 2 | Validation of the solid screening based on the *ortho*-xylylenediamine assay.** HEWT WT against no amino acceptor (control), 10 mM pyruvate, and 10 mM acetophenone in phosphate buffer pH 8, 10% (v/v) DMSO, room temperature. Pictures have been taken after 5 minutes, 1 and 2 hours, time when the darkening due to background starts to appear.



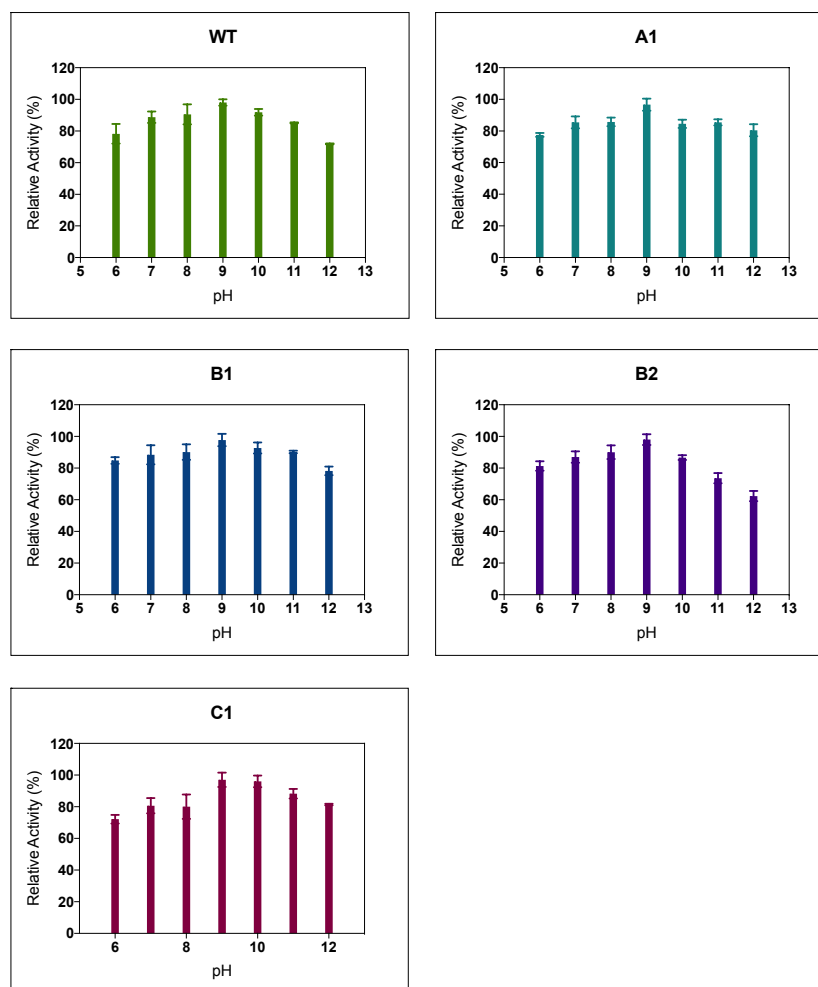
**Supplementary Figure 3 | Validation of the alternative reporter 4-nitrophenethylamine.** HEWT WT test using 10 mM 4-nitrophenethylamine as colour reporter against no exogeneous amino acceptor, in phosphate buffer pH 8, room temperature, when the background depletion step (Supplementary Fig. 1E) is or is not performed. Pictures show the progress of the colour changing along the time, at 30 min, 5 and 24 hours after incubation.



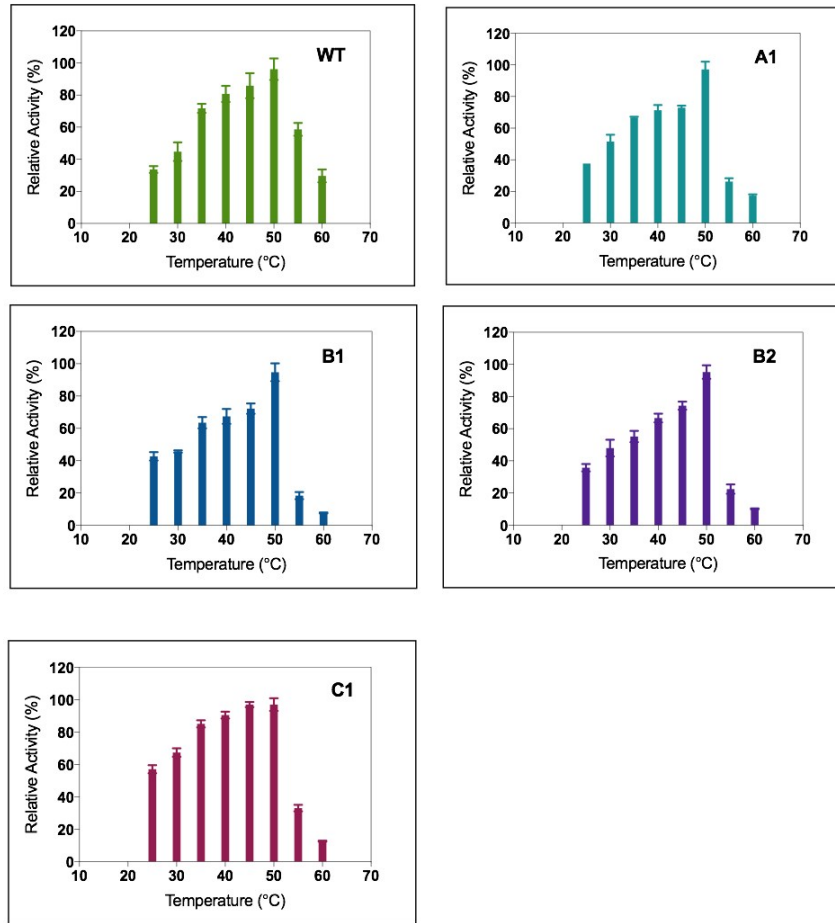
**Supplementary Figure 4 | The use of alternative amine donors during the depletion step.** HEWT WT test using 10 mM *ortho*-xylylenediamine as colour reporter against no exogeneous amino acceptor, in phosphate buffer pH 8, room temperature, with isopropylamine (50 mM), 1-phenylethylamine (10 mM, 1% DMSO (v/v)) or cadaverine (10 mM) during the background depletion step (Supplementary Fig. 1E) and without background depletion. Pictures show the progress of the colour changing along the time, at 3 and 24 hours after incubation.



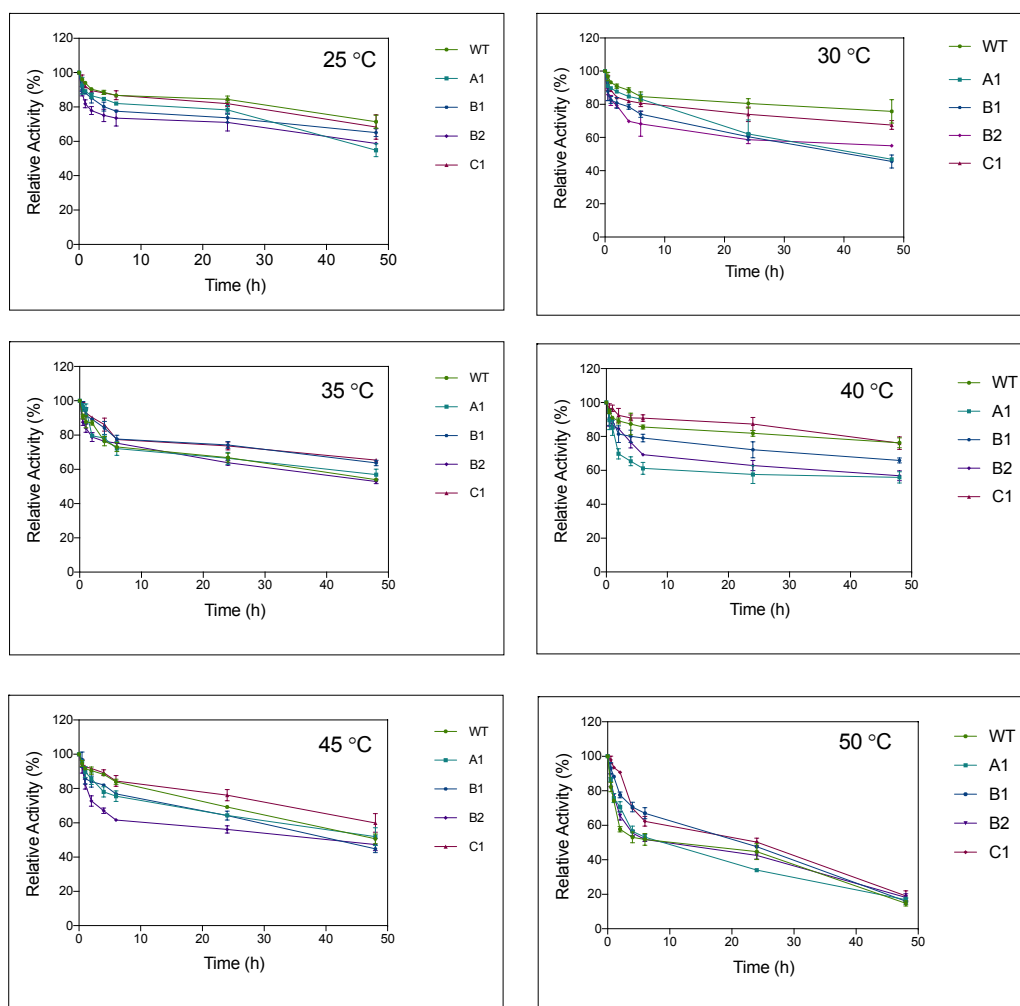
**Supplementary Figure 5 | pH effect on enzyme activity.** Activity experiments were performed in universal buffer at the desired pH (from pH 6 – 12) according to the standard activity assay described above.<sup>3</sup> The formation of acetophenone was quantified at 245 nm. 100 % activity corresponds to 4.0 U/mg, 0.98 U/mg, 1.2 U/mg, 1.3 U/mg, and 6.6 U/mg respectively. All measurements were performed in triplicate.



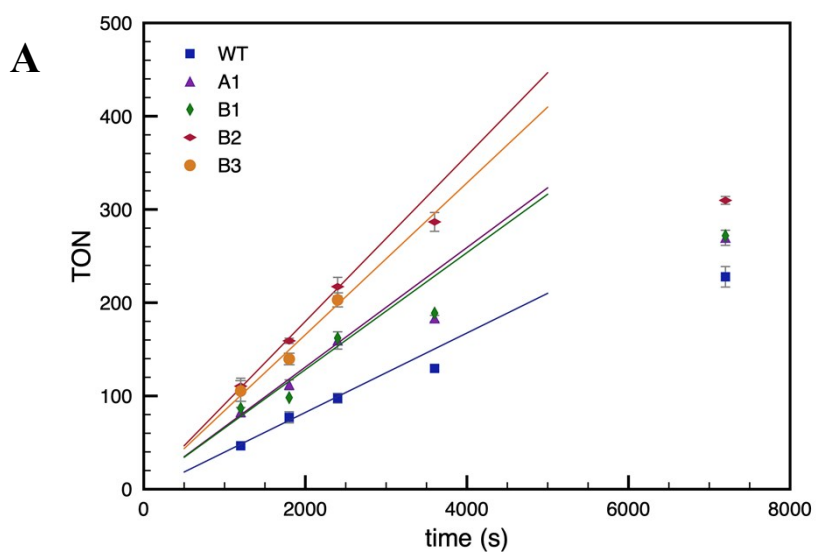
**Supplementary Figure 6 | pH effect on enzyme stability.** Purified enzyme was diluted with universal buffer at the desired pH (from pH 6 – 12) and stored at 4°C for 60 min. After incubation, the residual activity was determined using the standard enzyme activity assay described above. The formation of acetophenone was quantified at 245 nm. 100 % activity corresponds to 1.3 U/mg, 0.86 U/mg, 1.06 U/mg, 0.73 U/mg, 2.9 U/mg respectively. All measurements were performed in triplicate.

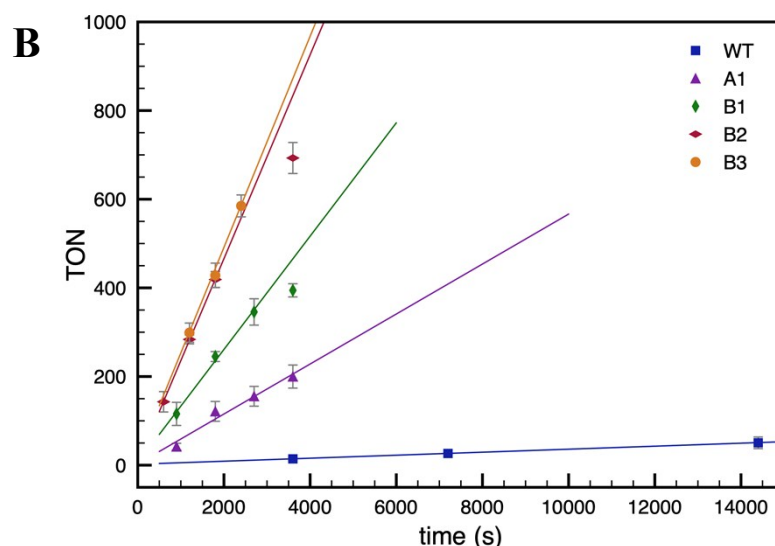


**Supplementary Figure 7 | Temperature effect on enzyme activity.** The activity was determined using the standard activity assay performed at the indicated temperature (from 25 °C - 60 °C). 100 % activity corresponds 4.8 U/mg, 2.35 U/mg, 2.5 U/mg and 6.9 U/mg respectively. All measurements were performed in triplicate.

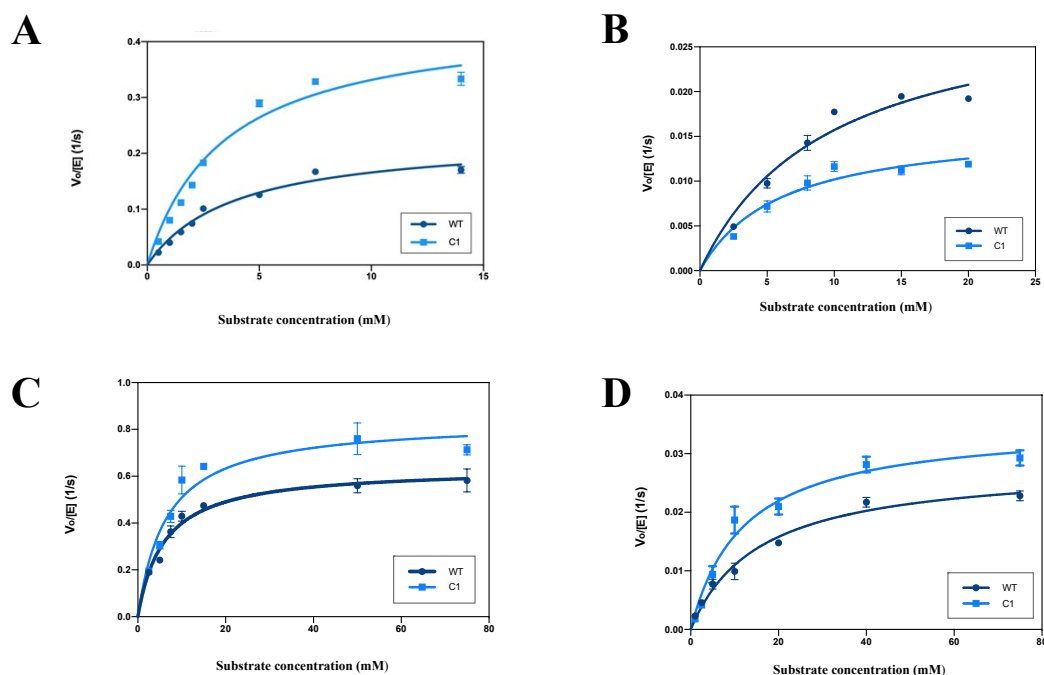


**Supplementary Figure 8 | Temperature effect on enzyme stability.** For the stability experiment, the enzyme was stored in phosphate buffer (50 mM pH 8.0) in the presence of pyridoxal 5'-phosphate (PLP) 1 mM and incubated at the desired temperature for up to 24 hours. The residual activity was determined using the standard activity assay. Acetophenone formation was quantified at 245 nm. 100 % activity corresponds to 4.0 U/mg, 0.8 U/mg, 1.3 U/mg, 1.3 U/mg and 4.5 U/mg respectively. All measurements were performed in triplicate.



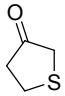
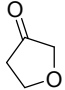
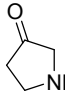
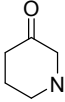


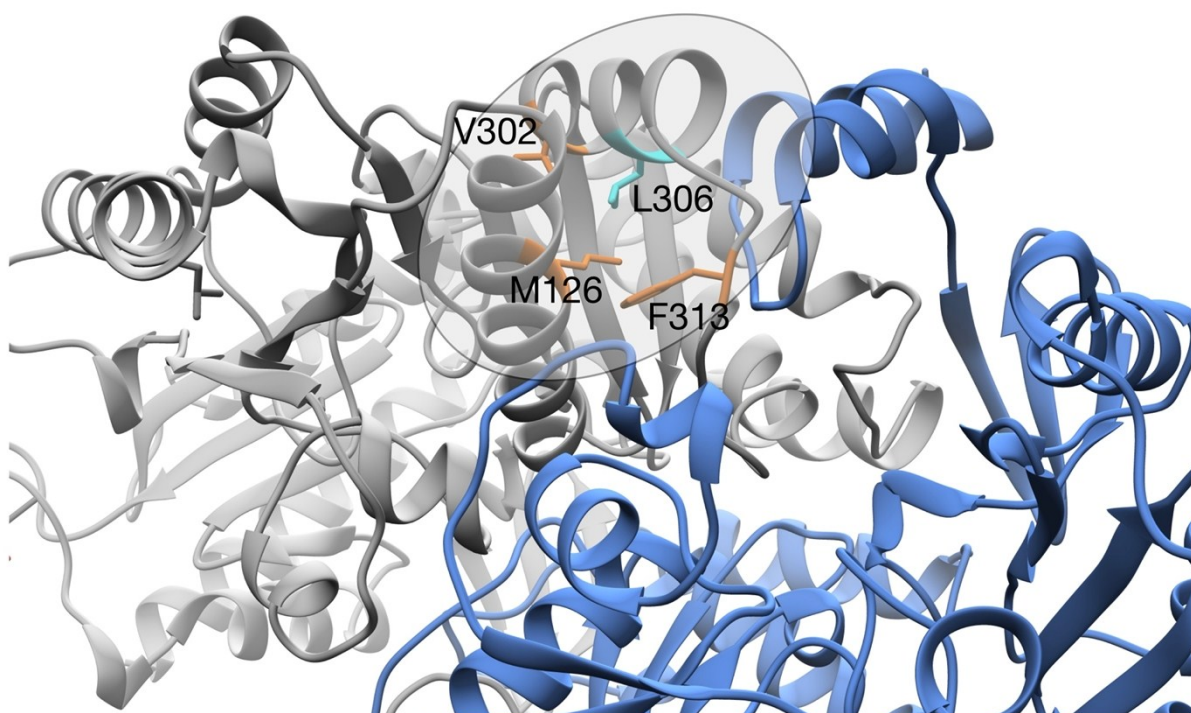
**Supplementary Figure 9 | Determination of TOF.** Turn over frequency (TOF) plot of WT and mutants A1, B1, B2, B3 for substrate (A) *para*-nitroacetophenone and (B) *para*-cyanoacetophenone. Reactions were performed in phosphate buffer (50 mM, pH 8.0, 10% (v/v) DMSO), containing 10 mM of the ketone substrate, 50 eq. of L-alanine, 0.1 mM PLP and 0.1 mg/mL (1.9  $\mu$ M).



**Supplementary Figure 10 | Determination of kinetic parameters.** Michaelis-Menten plot of WT (circles) and C1 mutant (triangles) for (A) tetrahydrothiophen-3-one, (B) tetrahydrofuran-3-one, (C) 1-methyl-3-pyrrolidinone and (D) 1-methyl-3-piperidinone; the initial-velocities were measured at pH 8.0 and 30  $^{\circ}$ C using the enzymatic kinetic assay detailed above. Reactions were carried out in the presence of 5 mM (S)-(-)-1-phenylethylamine (saturating conditions), various concentrations of the carbonyl substrate (0.5 - 75 mM), 0.25% DMSO, 0.1 mM PLP and an appropriate amount of the purified enzyme.

**Supplementary Table 1 | Kinetic Parameters.** Summary of the maximum turn-over frequency ( $k_{cat}$ ), Michaelis-Menten constant ( $K_M$ ), and catalytic efficiency of the HEWT ( $k_{cat}/K_M$ ).

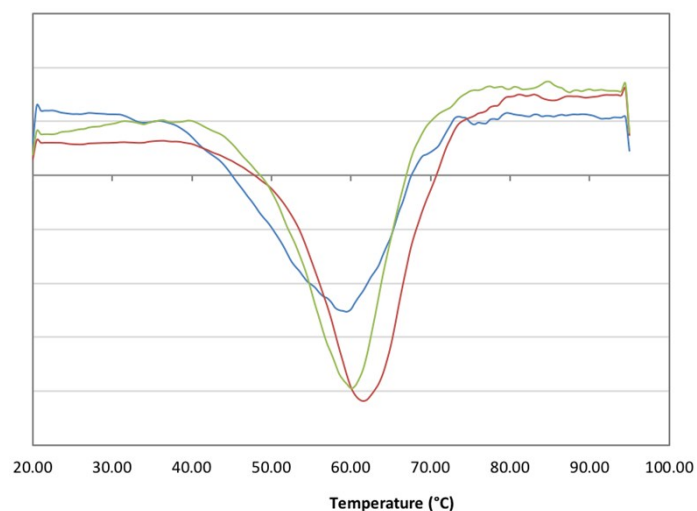
Substrate	WT			C1		
	$k_{cat}$ ( $10^{-3} \text{ s}^{-1}$ )	$K_M$ (mM)	$k_{cat}/K_M$ ( $10^{-3} \text{ s}^{-1} \text{ mM}^{-1}$ )	$k_{cat}$ ( $10^{-3} \text{ s}^{-1}$ )	$K_M$ (mM)	$k_{cat}/K_M$ ( $10^{-3} \text{ s}^{-1} \text{ mM}^{-1}$ )
 <b>3a</b>	230 ± 10	3.9 ± 0.4	60 ± 7	450 ± 40	3.4 ± 0.7	130 ± 3
 <b>4a</b>	620 ± 20	5.6 ± 0.5	101 ± 11	840 ± 40	6.5 ± 0.9	130 ± 20
 <b>5a</b>	30 ± 3	10 ± 2	3.0 ± 0.6	20 ± 1	6 ± 1	3.0 ± 0.6
 <b>6a</b>	30 ± 1	16 ± 2	2.0 ± 0.2	40 ± 2	12 ± 2	3.0 ± 0.4
All experiments were conducted in triplicate and the standard error is reported accordingly. For the determination of kinetics parameters, ketone concentrations between 0.5 and 75 mM were tested.						



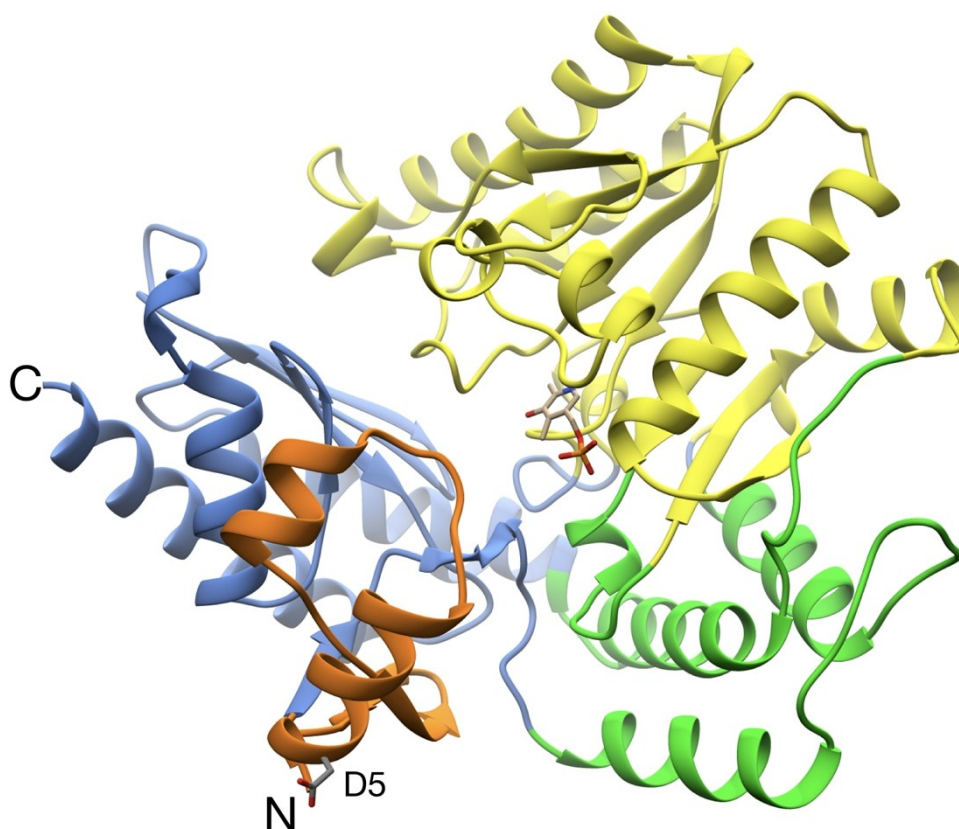
**Supplementary Figure 11 | Location of the L306M mutation on the HEWT crystal structure.** Cartoon representation of HEWT, focusing on the dimer interface. Mutation L306 to methionine may result in the formation of additional hydrophobic interactions with neighbouring hydrophobic residues (orange sticks). This



hydrophobic cluster (shaded ovals) would thus stabilise the dimer interface. This figure was generated using Chimera.<sup>13</sup>



**Supplementary Figure 12 | Thermal stability studies of HEWT WT, B2, C1.** First derivative of the thermal stability curves plotted in function of temperature. The melting temperature ( $T_m$ ) was calculated from the minimum of the derivative curves. HEWT WT 59 °C (blue line), B2 61 °C (red line), and C1 60 °C (green line).



**Supplementary Figure 13 | Domain composition of the HEWT crystal structure.** In order to identify regions that may be subject to structural fluctuations as independent rigid body units, chain A of HEWT was decomposed using the PiSQRD server software (<http://pisqrd.escience-lab.org>).<sup>14</sup> The subdivision of the crystal structure into four sub-domains is shown in ribbons. Domain 1 (residues 35-63, 262-267, 341-450; blue), Domain 2 (104-260, 268-282, 295-313), Domain 3 (residues 64-103, 112-115, 283-294, 314-340; green) and Domain 4 (residues 2-46; orange). D5 and PLP are shown in sticks. This figure was generated using Chimera.<sup>13</sup>



**Supplementary Table 2 | X-ray data collection, refinement and validation parameters.** Data were collected on a single HEWT crystal.  $R_{\text{merge}} = \sum |I - \langle I \rangle| / \sum I \times 100$ , where  $I$  is the intensity of a reflection and  $\langle I \rangle$  is the average intensity; Values in parentheses represent data belonging to highest resolution shells (2.0-2.05 Å).

HEWT WT	
<b>Data collection</b>	
Space group	P1
Cell dimensions	
$a, b, c$ (Å)	56.3 61.9 67.5
$\alpha, \beta, \gamma$ (°)	83.4, 82.6, 72.5
Resolution (Å)	40-2.0
$R_{\text{merge}}$	0.104 (0.42)
$I / \sigma$	8.5 (2.4)
No. unique reflections	54196 (3885)
Completeness (%)	93.4 (90.7)
Redundancy	1.7 (1.6)
<b>Refinement</b>	
Resolution (Å)	40 - 2.0
$R_{\text{work}} / R_{\text{free}}$ (%)	16/21
<i>No. atoms</i>	
Protein	13701
PLP	44
Water	159
Chloride ion	10
Ethylene glycol	10
<i>B-factors (Å<sup>2</sup>)</i>	
Protein	33.3
PLP	24.2
Water	27.0
Chloride ion	96.4
Ethylene glycol	45.2
<i>R.m.s. deviations</i>	
Bond lengths (Å)	0.003
Bond angles (°)	0.72
<i>Ramachandran Plot (%)</i>	
Favoured Regions	96.9
Allowed Regions	99.8

## Supplementary Notes

Wild-type HEWT sequence:

MRGSHHHHHGMASMTGGQQMGRDLYENLYFQGMQTQDYQALDRAHHLHPFTDFKALGEEGSRVVTHAEGVYIH  
DSEGNRILDGMAGLWCNVNLGYGRRELVEAATAQLEQLPYNTFFKTTHTPPAVRLAEKLCDLAPAHINRVFFTGSGSEAND  
TVLRMVERRYWALKGQPDQWIIIGRENAYHGSTLAGMSLGGMAPMHAQGGPCVPGIAHIRQPYWFGEGRDMSPFAF  
GQTCAEALEEKILELGEEKVAAFIAEPVQGAGGAIMPPESYWPAVKKVLAKYDILLVADEVICGFGRLEWFGSQHYGLEP  
DLMPIAKGLSSGYLPIGGVLVGDRVAETLIEEGGEFFHGFTYSGHPTCAAVALKNLELLEAEGVVDVRDRLGPLYAERWA  
SLVDHPVIGEARSLGLMGALELVADKTTGQRFDKSLGAGNLCRDLCFANGLVMRSVGDTMIISPLVIRREEIDELVELAR  
RALDETARQLTQVPHTQEEPTA

### Mutants:

A1: W56C, V435A

B1: W56C, L211V, L306M

B2: W56C, L211V, L306M, V361A, Q388R, P453L

B3: W56C, L211V, A254V, L306M, V361A, Q388R, P453L

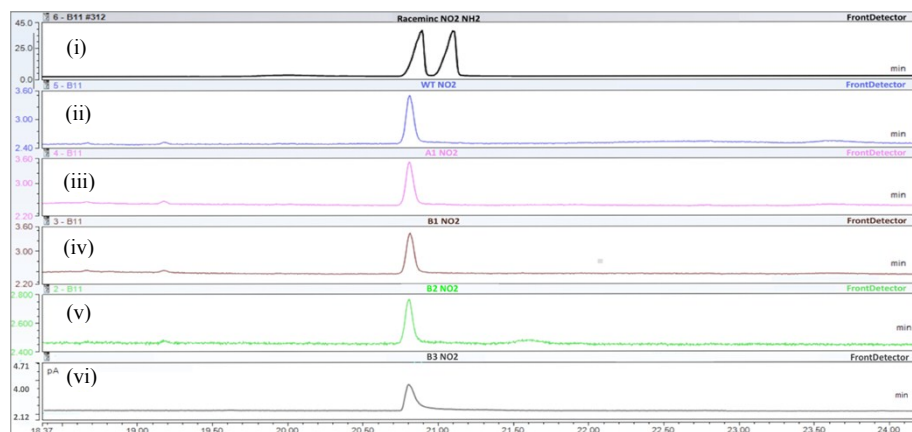
C1: D5E

## Supplementary References

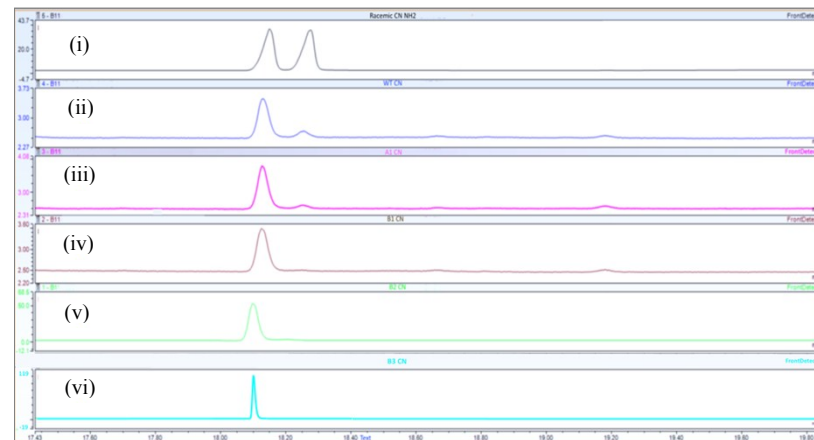
1. Cerioli, L., Planchestainer, M., Cassidy, J., Tessaro, D. & Paradisi, F. Characterization of a novel amine transaminase from *Halomonas elongata*. *J. Mol. Catal. B Enzym.* **120**, 141–150 (2015).
2. Studier, F. W. Protein production by auto-induction in high-density shaking cultures. *Protein Expr. Purif.* **41**, 207–234 (2005).
3. Schätzle, S., Höhne, M., Redestad, E., Robins, K. & Bornscheuer, U. T. Rapid and sensitive kinetic assay for characterization of  $\omega$ -transaminases. *Anal. Chem.* **81**, 8244–8248 (2009).
4. Svensson, O., Malbet-Monaco, S., Popov, A., Nurizzo, D. & Bowler, M. W. Fully automatic characterization and data collection from crystals of biological macromolecules. *Acta Crystallogr. Sect. D Biol. Crystallogr.* **71**, 1757–1767 (2015).
5. Bowler, M. W. *et al.* MASSIF-1: A beamline dedicated to the fully automatic characterization and data collection from crystals of biological macromolecules. *J. Synchrotron Radiat.* **22**, 1540–1547 (2015).
6. Kabsch, W. XDS. *Acta Cryst.* **D66**, 125–132 (2010).
7. Evans, P. R. Scaling and assessment of data quality. *Acta Cryst.* **D62**, 72–82 (2006).
8. Evans, P. R. An introduction to data reduction: Space-group determination, scaling and intensity statistics. *Acta Crystallogr. Sect. D Biol. Crystallogr.* **67**, 282–292 (2011).
9. Wilding, M., Scott, C., Newman, J. & Peat, T. S. Crystal structure of a putrescine aminotransferase from *Pseudomonas* sp. strain AAC. *Acta Crystallogr. Sect. Struct. Biol. Commun.* **73**, 29–35 (2017).
10. Emsley, P. & Cowtan, K. Coot: Model-building tools for molecular graphics. *Acta Crystallogr. Sect. D Biol. Crystallogr.* **60**, 2126–2132 (2004).
11. Adams, P. D. *et al.* A comprehensive Python-based system for macromolecular structure solution. *Acta Cryst.* **66**, 213–221 (2010).
12. Weiß, M. S., Pavlidis, I. V., Vickers, C., Hohne, M. & Bornscheuer, U. T. Glycine oxidase based high-throughput solid-phase assay for substrate profiling and directed evolution of (R)- and (S)-selective amine transaminases. *Anal. Chem.* **86**, 11847–11853 (2014).
13. Pettersen, E. F. *et al.* UCSF Chimera?A visualization system for exploratory research and analysis. *J. Comput. Chem.* **25**, 1605–1612 (2004).
14. Aleksiev, T., Potestio, R., Pontiggia, F., Cozzini, S. & Micheletti, C. PiSQRD: a web server for decomposing proteins into quasi-rigid dynamical domains. *Bioinformatics* **25**, 2743–2744 (2009).

## GC-FID Chromatograms

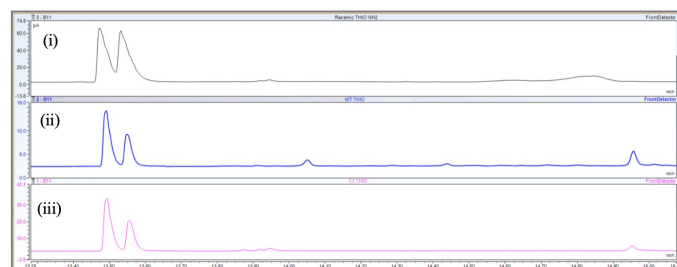
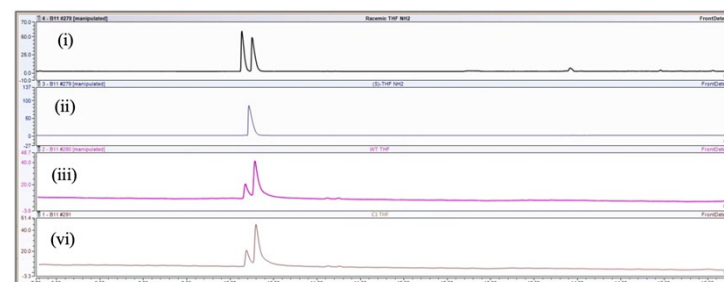
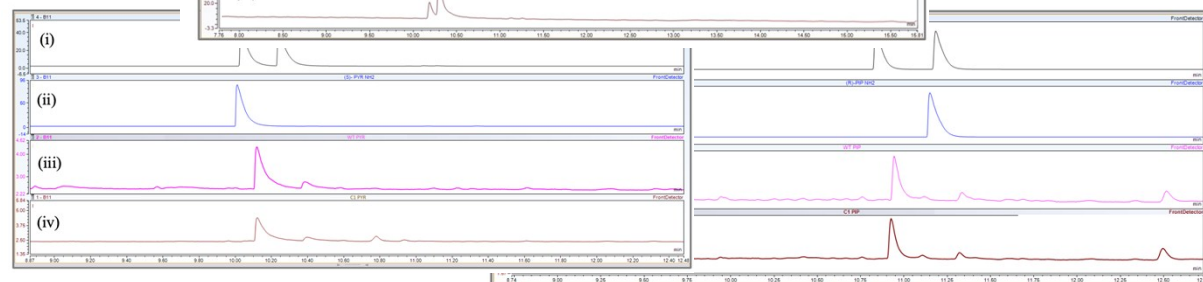
**A**



**B**



**GC-FID analysis of aromatic amines | (A)** Determination of *e.e.* following biotransformation with *wild-type* HEWT and the best mutant variants evolved towards *para*-NO<sub>2</sub>-acetophenone. The enantiomeric purity of (*S*)-*para*-NO<sub>2</sub>-phenylethylamine was determined by comparison with commercially available standards: **(i)** *para*-NO<sub>2</sub>-phenylethylamine; **(ii)** *wild-type* HEWT biotransformation trace; **(iii)** A1 variant biotransformation trace; **(iv)** B1 variant biotransformation trace; **(v)** B2 variant biotransformation trace; **(vi)** B3 variant biotransformation trace **(B)** Determination of *e.e.* following biotransformation with *wild-type* HEWT and the best mutant variants evolved towards *para*-CN-acetophenone. The enantiomeric purity of (*S*)-*para*-CN-phenylethylamine was determined by comparison with commercially available standards: **(i)** *para*-CN-phenylethylamine, **(ii)** *wild-type* HEWT biotransformation trace; **(iii)** A1 variant biotransformation trace; **(iv)** B1 variant biotransformation trace; **(v)** B2 variant biotransformation trace; **(vi)** B3 variant biotransformation trace.

**A****B****C**

**GC-FID analysis of cyclic amines | (A)** Determination of *e.e.* following biotransformation of tetrahydrothiophen-3-one with *wild-type* HEWT and the C1 variant. Enantiomeric purity was determined by comparison with commercially available standards: **(i)** tetrahydro-3-thienylamine; **(ii)** *wild-type* HEWT biotransformation trace; **(iii)** C1 variant biotransformation trace. **(B)** Determination of *e.e.* following biotransformation of tetrahydrofuran-3-one with *wild-type* HEWT and the C1 variant. Enantiomeric purity was determined by comparison with commercially available standards; **(i)** tetrahydrofuran-3-amine; **(ii)** (*S*)-tetrahydrofuran-3-amine; **(iii)** *wild-type* HEWT biotransformation trace; **(iv)** C1 variant biotransformation trace. **(C)** Determination of *e.e.* following biotransformation of 1-methyl-3-pyrrolidinone with *wild-type* HEWT and the C1 variant. Enantiomeric purity was determined by comparison with commercially available standards; **(i)** 1-methylpyrrolidin-3-amine; **(ii)** (*S*)-1-methylpyrrolidin-3-ylamine; **(iii)** *wild-type* HEWT biotransformation trace; **(iv)** C1 variant biotransformation trace. **(D)** Determination of *e.e.* following biotransformation of 1-methyl-3-piperidinone with *wild-type* HEWT and the C1 variant. Enantiomeric purity was determined by comparison with commercially available standards; **(i)** 1-methyl-piperidin-3-ylamine; **(ii)** (*R*)-1-methyl-piperidin-3-ylamine, **(iii)** *wild-type* HEWT biotransformation trace; **(iv)** C1 variant biotransformation trace.